JACS
JOURNAL OF THE AMERICAN CHEMICAL SOCIETY
Communication
pubs.acs.org/JACS

Microporous Brookite-Phase Titania Made by Replication of a Metal–Organic Framework

Anthony Shoji Hall,[†] Atsushi Kondo,*[,‡] Kazuyuki Maeda,[‡] and Thomas E. Mallouk*[,†]

[†]Department of Chemistry, The Pennsylvania State University, University Park, Pennsylvania 16802, United States
[‡]Department of Applied Chemistry, Graduate School of Engineering, Tokyo University of Agriculture and Technology, 2-24-16 Naka-cho, Koganei, Tokyo 184-8588, Japan

Supporting Information

ABSTRACT: Metal–organic frameworks (MOFs) provide access to structures with nanoscale pores, the size and connectivity of which can be controlled by combining the appropriate metals and linkers. To date, there have been no reports of using MOFs as templates to make porous, crystalline metal oxides. Microporous titania replicas were made from the MOF template HKUST-1 by dehydration, infiltration with titanium isopropoxide, and subsequent hydrothermal treatment at 200 °C. Etching of the MOF with 1 M aqueous HCl followed by 5% H_2O_2 yielded a titania replica that retained the morphology of the parent HKUST-1 crystals and contained partially ordered micropores as well as disordered mesopores. Interestingly, the synthesis of porous titania from the HKUST-1 template stabilized the formation of brookite, a rare titania polymorph.

A variety of templating strategies using surfactants,[1−4] block copolymers,[5−7] colloidal crystals,[8−11] mesoporous silica,[12,13] and zeolites[14−16] have been developed for the synthesis of porous materials with controlled pore dimensions. These techniques generally rely on infiltration of porous solids[7−15] or solution-phase co-assembly of soft templates with precursor reagents;[1−6] the template is removed by chemical etching or calcination if the sample is a hard or soft template, respectively. These methods have provided a means of controlling the pore wall thickness, pore periodicity, pore diameter, and pore connectivity in thin films and nanoparticulate materials.

Porous metal oxides are now the subject of intense interest because of their uses in photocatalysis,[17−20] electrochemical energy storage,[21,22] and heterojunction photovoltaics.[23−25] High surface area and crystallinity are vital to the performance of oxides in these applications.[20−26] While high surface area crystalline metal oxides can be prepared with ordered mesopores, it is still a significant challenge to make crystalline metal oxide particles that contain ordered micropores.[17] Nanocomposites of amorphous metal oxides and microporous or mesoporous organic templates can be synthesized quite easily; however, the high temperatures needed to crystallize the amorphous oxide and remove the soft template result in collapse and sealing of the micropores, because degradation of the template and grain growth occur simultaneously.[17] Metal oxides prepared by these templating methods have pore diameters that range from 0.48 to 50 nm.[3,27−29] However, the micropores in these replicated materials in general do not have any ordering derived from the template.[40−45]

Metal–organic frameworks (MOFs) or porous coordination polymers are solids that offer control of pore size and geometry by selecting the appropriate molecular building units.[30−37] Recently there have been several reports of using MOFs as precursor materials to high surface area graphitic carbon, which is made by infiltration with a carbon precursor followed by calcination[38−40] or by direct decomposition of the MOF. In neither case do the carbon replicas show evidence of pore ordering that is derived from the MOF template.[41−43] There have also been many reports of the synthesis of nonporous metal and metal oxide nanoclusters and nanoparticles within the pores of zeolites and MOFs.[44−49] More recently, there have been some reports of porous metal oxides made by direct calcination of MOFs that contain the metal of interest from the framework; again the sizes and connectivity of pores in these oxides are not derived directly from the pore structure of the MOFs.[50−52]

Here we report the synthesis of a crystalline metal oxide with a micro-meso binary pore system from a MOF template. The micropores in this material are derived from the MOF template and are partially ordered. The mesopores are generated by incomplete filling of the template. For this initial study we chose titania as a model system. Interestingly, phase pure brookite, a rare titania polymorph that is otherwise difficult to prepare in pure form,[53,54] results from replication of the copper-based MOF, HKUST-1.[55]

Porous titania replicas of HKUST-1 were prepared by liquid-phase impregnation under vacuum as illustrated in Figure 1. HKUST-1 was prepared as described elsewhere with minor modifications.[55,56] In a typical procedure, 2.0 g of the HKUST-1 template was heated overnight at 200 °C in vacuum in a Schlenk flask. After cooling the flask to room temperature, 10 mL of titanium(IV) isopropoxide, Ti(O-*i*Pr)$_4$ (96% Sigma Aldrich),

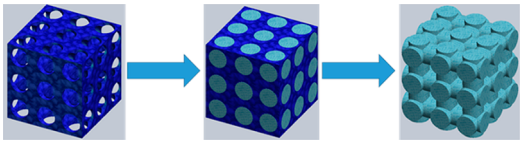

Figure 1. Schematic illustration of the synthesis of microporous brookite from a MOF template.

Received: August 11, 2013
Published: October 17, 2013

dx.doi.org/10.1021/ja4083254 | J. Am. Chem. Soc. 2013, 135, 16276−16279

was injected directly over the powder. This represents a large excess; preliminary experiments with 400 μL Ti(O-*i*Pr)$_4$ per gram of HKUST-1 gave hollow pyramidal structures. The Schlenk flask was kept under dynamic vacuum for 30 min after injection of Ti(O-*i*Pr)$_4$. The HKUST-1 was kept immersed in the liquid Ti(O-*i*Pr)$_4$ for a minimum of 24 h under static vacuum to allow the precursor molecules to infiltrate into the pores. The sample was then removed from the Schlenk flask, washed, and centrifuged with ethanol three times to remove excess Ti(O-*i*Pr)$_4$. The powder was redispersed in ethanol and filtered and washed with additional ethanol. The washing step with ethanol is critical for removing Ti(O-*i*Pr)$_4$ from the surface of the MOF particles. The dried powder was suspended in 10 mL of a mixture of ethanol and water (1:1 by volume), placed in a 23 mL Teflon-lined stainless steel autoclave, and heated for 20 h at 200 °C. After this hydrothermal treatment, the sample was filtered. The resulting powder was placed in 1 M HCl to etch the HKUST-1 template, then filtered, and washed with water. The powder was then subjected to a second etch with 5 wt % H_2O_2. Finally the solution was filtered and washed with water and ethanol resulting in a porous crystalline titania powder. The titania replica derived from HKUST-1 is denoted as MT1. Without the hydrothermal treatment step, we obtained only amorphous titania.

Figure 2a,b shows SEM images of the HKUST-1 template and of HKUST-1/titania composite particles after hydrothermal

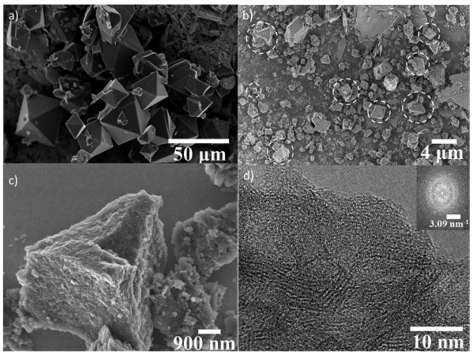

Figure 2. FESEM images showing (a) bipyramidal crystals of the HKUST-1 template and (b) the composite after the hydrothermal treatment but before etching. The white dotted lines highlight particles that retain the morphology of the HKUST-1 crystals. (c) Porous titania (MT1) after removal of the HKUST-1 template. (d) High-resolution TEM image of MT1. The inset shows a FFT of the image. The rings in the inset correspond to the average pore spacing (1.0 nm) and the brookite (111) and (120) lattice spacings of 0.33 nm.

treatment (henceforth denoted as the composite) that retain the square bipyramidal shape of the HKUST-1 crystals. Many of the composite particles consist of fractured pieces derived from the template. Although these fractured particles do not show the macroscale morphology of the MOF crystals, they do contain the same nanostructured porosity. Figure 2c shows a SEM image of porous titania (MT1) obtained after HKUST-1 template removal. Some of the MT1 particles retain the square bipyramidal shape of the HKUST-1 crystals. SEM images at higher magnification (Figure SI-1) show that the pyramidal MT1 particles consist of smaller particles that appear fibrous and porous on their surface. Figure 2d shows a high-resolution TEM image of MT1. Disordered micropores with uniform spacing are evident in the sample. A fast Fourier transform (FFT) of the boxed region in Figure 2d indicates that the average spacing of the pores is 1.0 nm. Lattice fringes with 0.33 nm spacing, attributed to the brookite phase of titania, are also seen in the image and the FFT.

The Ti/Cu molar ratio measured by atomic absorption spectroscopy was 9.6, indicating that the etched sample consists predominantly of titanium dioxide. TGA (Figure SI-2) shows that MT1 contains of <5 wt % carbon.

Figure 3 shows high resolution XPS of MT1, HKUST-1, and the composite. HKUST-1 contains Cu^{2+} (Figure 3a) as indicated

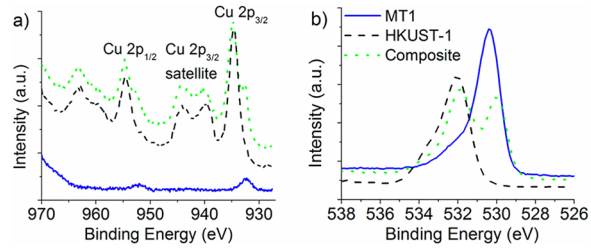

Figure 3. High-resolution XPS scans of MT1, HKUST-1 template, and the composite after crystallization. Normalized (a) copper and (b) oxygen spectra.

by the position of the Cu 2p$_{1/2}$, Cu 2p$_{3/2}$, and Cu^{2+} satellite peaks.[57] XPS shows the presence of residual Cu^+-O bonds in MT1, indicated by the Cu 2p$_{3/2}$ peak at 932 eV and the Cu 2p$_{1/2}$ peak at 952 eV (Figure 3a).[58] The XPS spectra in Figure 3a show the presence of both Cu^{2+} and Cu^+ in the composite; this indicates that hydrothermal crystallization partially reduces copper in the template. It is likely that the copper impurity present in the sample is amorphous Cu_2O, which is formed by reduction of Cu^{2+}. The XPS spectra in Figure SI-3 show Ti 2p$_{1/2}$ and Ti 2p$_{3/2}$ peaks centered at ~465 and ~459 eV, respectively, indicating that both samples contain the Ti^{4+}-O bonds of TiO_2.[58] The O 1s XPS spectrum of HKUST-1 in Figure 3b shows a major peak at a binding energy of ~532 eV and a small shoulder at ~534 eV, which confirm the presence of carboxyl and ester groups, respectively.[59] The O 1s XPS spectrum of the composite shows peaks at ~532, ~534, and 530 eV which indicate that the sample contains carboxyl, ester, and Ti-O bonds. The XPS spectrum of MT1 shows a major peak at a binding energy of ~530.5 eV, which indicates the presence of Ti-O bonds.[58,59] After etching, the peak corresponding to the Ti-O bond shifts slightly to 530.5 eV, suggesting that template removal causes a change in the bonding environment of Ti. The peaks corresponding to ester and carboxyl groups are not present in MT1, confirming that the HKUST-1 template is completely removed. The carbon species present in the sample could not be identified because the carbon signal from MT1 could not be differentiated from background adventitious carbon.

XRD patterns were recorded to follow the progression of crystalline phases formed in the reaction (Figure 4). The composite showed an identical XRD pattern (Figure SI-4) to that of the original HKUST-1 template, indicating that the composites are well ordered before template removal. The low-angle region of the XRD pattern of MT1 shows a large, broad peak centered at $2\theta = 8.4°$, which corresponds to a distribution of pore spacings centered at 1.06 nm ±0.4 nm. The pore spacing of MT1 determined by XRD is consistent with the results shown in Figure 2d. The TEM image shows lattice planes with ~0.33 nm periodicity corresponding to the (111) and (120) lattice planes of brookite phase titania. A simulated pattern of the HKUST-1 template shows three sharp diffraction peaks between 2θ = 5–12°, which correspond to the 200, 220, and 222 reflections. This

dx.doi.org/10.1021/ja4083254 | J. Am. Chem. Soc. 2013, 135, 16276–16279

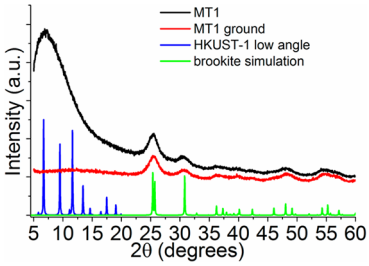

Figure 4. XRD patterns of porous titania (MT1) (black), MT1 after grinding in a mortar and pestle (red), HKUST-1 simulation (blue), and brookite phase titania (green).

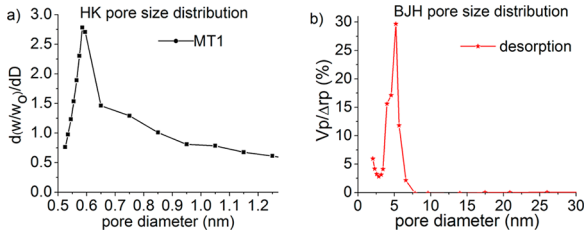

Figure 5. (a) HK micropore size distribution calculated from the N_2 adsorption isotherm for MT1 shown in Figure SI-6. (b) BJH mesopore size distribution of MT1 calculated from N_2 desorption isotherm shown in Figure SI-6.

suggests that pore ordering of MT-1 is derived from the HKUST-1 template, albeit with greater disorder. Figure 4 also shows XRD data collected after MT1 was ground with a mortar and pestle. The disappearance of the low angle peak indicates the loss of pore order with grinding. The diffraction peaks of MT1 at higher angles, which can be attributed to nanocrystalline brookite, are not affected by grinding. We investigated the effect of solvents and temperature during the crystallization step; XRD patterns confirmed that phase pure brookite was formed under a range of different conditions (Figure SI-5). Under the hydrothermal conditions used in this study anatase or rutile phase titania are most typically formed. The formation of phase pure brookite in the case of the HKUST-1 template most likely arises from the presence of Cu^{2+} ions as noted in previous reports.[54]

The dehydrated HKUST-1 template contains square-shaped pores of ~1.0 nm diameter.[55,60] This is comparable to the van der Waals diameter of the flexible $Ti(O\text{-}iPr)_4$ molecule which was estimated using ChemDraw as 0.99 nm. The average micropore diameter of the titania replica is smaller than the value expected from replication of the MOF framework. The smaller dimensions can be attributed to volume shrinkage of the infiltrated titania upon condensation and crystallization.

The porosity of the samples was analyzed by nitrogen gas adsorption−desorption isotherms at 77 K (Figure SI-6). The adsorption−desorption isotherms of MT1 show typical type IV behavior.[61] The steep uptake at low relative pressure indicates the presence of micropores. The micropore volume and isosteric heat of adsorption derived from N_2 adsorption by Dubinin−Radushkevich analysis[62] are 0.090 mL/g and 10.8 kJ/mol, respectively. The Horvath−Kawazoe (HK) method[63] was used to fit the adsorption isotherm and obtain the micropore size distribution. The graph in Figure SI-7b shows that MT1 (HCl etched only) has a relatively broad distribution of micropore diameters with a maximum frequency near 0.52 nm. Figure 5a shows that after H_2O_2 etching the micropore distribution of MT1 becomes more uniform, and additionally the maximum frequency of the micropore diameter increases to 0.60 nm.

A hysteresis loop in the adsorption−desorption isotherm was observed at higher pressures indicating the presence of mesopores (Figures SI-6 and SI-7a). The mesopore volume was calculated as 0.23 mL/g from the micropore volume and total pore volume near $P/P_0 = 1$. To measure the mesopore distribution, Barrett−Joyner−Halenda (BJH) theory[64] was applied to the desorption branch of the isotherm. This analysis indicates that the mesopore diameter in MT1 is centered around 6 nm. The mesopore distribution calculated from the adsorption branch is presented in Figure SI-6. The Brunauer−Emmett−Teller surface area[65] of MT1 was in the range 180−190 m^2/g after HCl etching but before H_2O_2 etching. After H_2O_2 etching the surface area increased to 265−270 m^2/g.

The broad distribution of both micro- and mesopores is likely caused by incomplete filling of the HKUST-1 template with titania. The volume shrinkage during crystallization and solvent elimination during hydrolysis makes it difficult to completely fill the small pores with titania. Based on the N_2 adsorption experiment, we measured a micropore volume of 0.49 mL/g for the HKUST-1 template. From the pore volume of HKUST-1 and the brookite density (4.1 g/cm^3), we can estimate that a completely filled composite should have a Ti/Cu ratio of 5.3. The Ti/Cu ratio of the composite was found to be 1.4 by XPS, indicating only partial pore filling. A N_2 adsorption experiment on the composite (Figure SI-9) gave a micropore volume of 0.23 mL/g, which is almost the half that of HKUST-1. This is also consistent with only partial filling of the pores in the composite by titania. From the framework volume of HKUST-1 and the density of brookite, a perfect titania replica should have a micropore volume of 0.36 mL/g. This is close to the total pore volume (0.09 micropore + 0.23 mesopore = 0.32 mL/g) we observe in the replica. This suggests that partial collapse of micropores in the imperfect replica gives rise to an equivalent mesopore volume.

In summary, we demonstrate a simple method of synthesizing high surface area micro/mesoporous brookite phase titania with surface areas up to 270 m^2/g by using HKUST-1 as a template. The porous particles have micropore diameters and pore spacings that are derived from the MOF template. The mesopores appear to arise from incomplete filling of the pores of the template by $Ti(O\text{-}iPr)_4$. Because many metal oxides can be crystallized hydrothermally from metal alkoxide precursors, it is likely that other microporous oxides can be synthesized by the same technique. Further work is underway to determine the range of compositions and stability of porous oxides that can be made by replication of MOFs.

■ ASSOCIATED CONTENT

Ⓢ Supporting Information

Experimental details and data. This material is available free of charge via the Internet at http://pubs.acs.org.

■ AUTHOR INFORMATION

Corresponding Authors

kondoa@cc.tuat.ac.jp
tem5@psu.edu

Notes

The authors declare no competing financial interest.

dx.doi.org/10.1021/ja4083254 | J. Am. Chem. Soc. 2013, 135, 16276−16279

■ ACKNOWLEDGMENTS

We thank Dong-Dong Qin (Lanzhou University), Stuart A. Friesen and Dimitri Vaughn (PSU) for helpful discussions. We thank Julie Anderson (PSU) and Lymaris Ortiz (PSU) for help with BET experiments. We also thank Ke Wang (PSU), Josh Maier (PSU), and Trevor Clark (PSU) for assistance with TEM. Work at Penn State was supported by the Office of Basic Energy Sciences, Division of Chemical Sciences, Geosciences, and Energy Biosciences, DOE under contract DE-FG02-07ER15911. A.K. was partly supported by the Institutional Program for Young Researcher Overseas Visits of the Japan Society for the Promotion of Science.

■ REFERENCES

(1) Yanagisawa, T.; Shimizu, T.; Kuroda, K.; Kato, C. *Bull. Chem. Soc. Jpn.* **1990**, *63*, 988.
(2) Beck, J. S.; Vartuli, J. C.; Roth, W. J.; Leonowicz, M. E.; Kresge, C. T.; Schmitt, K. D.; Chu, C. T. W.; Olson, D. H.; Sheppard, E. W.; Mccullen, S. B.; Higgins, J. B.; Schlenker, J. L. *J. Am. Chem. Soc.* **1992**, *114*, 10834.
(3) Ania, C. O.; Khomenko, V.; Raymundo-Pinero, E.; Parra, J. B.; Beguin, F. *Adv. Funct. Mater.* **2007**, *17*, 1828.
(4) Ji, L. L.; Liu, F. L.; Xu, Z. Y.; Zheng, S. R.; Zhu, D. Q. *Environ. Sci. Technol.* **2009**, *43*, 7870.
(5) Zhao, D. Y.; Feng, J. L.; Huo, Q. S.; Melosh, N.; Fredrickson, G. H.; Chmelka, B. F.; Stucky, G. D. *Science* **1998**, *279*, 548.
(6) Monnier, A.; Schuth, F.; Huo, Q.; Kumar, D.; Margolese, D.; Maxwell, R. S.; Stucky, G. D.; Krishnamurty, M.; Petroff, P.; Firouzi, A.; Janicke, M.; Chmelka, B. F. *Science* **1993**, *261*, 1299.
(7) Zimny, K.; Rogues-Cannes, T.; Carteret, C.; Stebe, M. J.; Blin, J. L. *J. Phys. Chem. C* **2012**, *116*, 6585.
(8) Zakhidov, A. A.; Baughman, R. H.; Iqbal, Z.; Cui, C. X.; Khayrullin, I.; Dantas, S. O.; Marti, I.; Ralchenko, V. G. *Science* **1998**, *282*, 897.
(9) Kulinowski, K. M.; Jiang, P.; Vaswani, H.; Colvin, V. L. *Adv. Mater.* **2000**, *12*, 833.
(10) Velev, O. D.; Kaler, E. W. *Adv. Mater.* **2000**, *12*, 531.
(11) Yu, J. S.; Kang, S.; Yoon, S. B.; Chai, G. *J. Am. Chem. Soc.* **2002**, *124*, 9382.
(12) Lee, J.; Yoon, S.; Hyeon, T.; Oh, S. M.; Kim, K. B. *Chem. Commun.* **1999**, 2177.
(13) Lee, J. S.; Joo, S. H.; Ryoo, R. *J. Am. Chem. Soc.* **2002**, *124*, 1156.
(14) Johnson, S. A.; Brigham, E. S.; Ollivier, P. J.; Mallouk, T. E. *Chem. Mater.* **1997**, *9*, 2448.
(15) Ma, Z. X.; Kyotani, T.; Tomita, A. *Chem. Commun.* **2000**, 2365.
(16) Lu, A. H.; Schuth, F. *Adv. Mater.* **2006**, *18*, 1793.
(17) Noda, Y.; Lee, B.; Domen, K.; Kondo, J. N. *Chem. Mater.* **2008**, *20*, 5361.
(18) Yu, J. G.; Zhao, X. J.; Zhao, Q. N. *Thin Solid Films* **2000**, *379*, 7.
(19) Sayama, K.; Sugihara, H.; Arakawa, H. *Chem. Mater.* **1998**, *10*, 3825.
(20) Wang, X. C.; Yu, J. C.; Ho, C. M.; Hou, Y. D.; Fu, X. Z. *Langmuir* **2005**, *21*, 2552.
(21) Sreethawong, T.; Suzuki, Y.; Yoshikawa, S. *Int. J. Hydrogen Energy* **2005**, *30*, 1053.
(22) Brezesinski, T.; Wang, J.; Polleux, J.; Dunn, B.; Tolbert, S. H. *J. Am. Chem. Soc.* **2009**, *131*, 1802.
(23) Oregan, B.; Gratzel, M. *Nature* **1991**, *353*, 737.
(24) Lee, M. M.; Teuscher, J.; Miyasaka, T.; Murakami, T. N.; Snaith, H. J. *Science* **2012**, *338*, 643.
(25) Crossland, E. J.; Noel, N.; Sivaram, V.; Leijtens, T.; Alexander-Webber, J. A.; Snaith, H. J. *Nature* **2013**, *495*, 215.
(26) Stone, V. F.; Davis, R. J. *Chem. Mater.* **1998**, *10*, 1468.
(27) Ren, Y.; Ma, Z.; Morris, R. E.; Liu, Z.; Jiao, F.; Dai, S.; Bruce, P. G. *Nat. Commun.* **2013**, *4*, 2015.
(28) Chaplais, G.; Schlichte, K.; Stark, O.; Fischer, R. A.; Kaskel, S. *Chem. Commun.* **2003**, 730.
(29) Rudisill, S. G.; Wang, Z. Y.; Stein, A. *Langmuir* **2012**, *28*, 7310.
(30) Hoskins, B. F.; Robson, R. *J. Am. Chem. Soc.* **1990**, *112*, 1546.
(31) Hagrman, D.; Hagrman, P. J.; Zubieta, J. *Angew. Chem., Int. Ed.* **1999**, *38*, 3165.
(32) Moulton, B.; Zaworotko, M. J. *Chem. Rev.* **2001**, *101*, 1629.
(33) Carlucci, L.; Ciani, G.; Proserpio, D. M. *Coord. Chem. Rev.* **2003**, *246*, 247.
(34) Zhou, H. C.; Long, J. R.; Yaghi, O. M. *Chem. Rev.* **2012**, *112*, 673.
(35) Horcajada, P.; Chalati, T.; Serre, C.; Gillet, B.; Sebrie, C.; Baati, T.; Eubank, J. F.; Heurtaux, D.; Clayette, P.; Kreuz, C.; Chang, J. S.; Hwang, Y. K.; Marsaud, V.; Bories, P. N.; Cynober, L.; Gil, S.; Ferey, G.; Couvreur, P.; Gref, R. *Nat. Mater.* **2010**, *9*, 172.
(36) Kitagawa, S.; Uemura, K. *Chem. Soc. Rev.* **2005**, *34*, 109.
(37) Kreno, L. E.; Leong, K.; Farha, O. K.; Allendorf, M.; Van Duyne, R. P.; Hupp, J. T. *Chem. Rev.* **2012**, *112*, 1105.
(38) Jiang, H. L.; Liu, B.; Lan, Y. Q.; Kuratani, K.; Akita, T.; Shioyama, H.; Zong, F.; Xu, Q. *J. Am. Chem. Soc.* **2011**, *133*, 11854.
(39) Liu, B.; Shioyama, H.; Akita, T.; Xu, Q. *J. Am. Chem. Soc.* **2008**, *130*, 5390.
(40) Meng, Y.; Wang, G. H.; Bernt, S.; Stock, N.; Lu, A. H. *Chem. Commun. (Cambridge, U. K.)* **2011**, *47*, 10479.
(41) Chaikittisilp, W.; Hu, M.; Wang, H. J.; Huang, H. S.; Fujita, T.; Wu, K. C. W.; Chen, L. C.; Yamauchi, Y.; Ariga, K. *Chem Commun* **2012**, *48*, 7259.
(42) Chaikittisilp, W.; Ariga, K.; Yamauchi, Y. *J. Mater. Chem. A* **2013**, *1*, 14.
(43) Torad, N. L.; Hu, M.; Kamachi, Y.; Takai, K.; Imura, M.; Naito, M.; Yamauchi, Y. *Chem. Commun.* **2013**, *49*, 2521.
(44) Turner, S.; Lebedev, O. I.; Schroder, F.; Esken, D.; Fischer, R. A.; Van Tendeloo, G. *Chem. Mater.* **2008**, *20*, 5622.
(45) Muller, M.; Zhang, X. N.; Wang, Y. M.; Fischer, R. A. *Chem. Commun.* **2009**, 119.
(46) Esken, D.; Zhang, X.; Lebedev, O. I.; Schroder, F.; Fischer, R. A. *J. Mater. Chem.* **2009**, *19*, 1314.
(47) Muller, M.; Lebedev, O. I.; Fischer, R. A. *J. Mater. Chem.* **2008**, *18*, 5274.
(48) Moon, H. R.; Kim, J. H.; Suh, M. P. *Angew. Chem., Int. Ed.* **2005**, *44*, 1261.
(49) Jacobs, B. W.; Houk, R. J. T.; Wong, B. M.; Talin, A. A.; Allendorf, M. D. *Nanotechnology* **2011**, *22*, 375601.
(50) Kim, T. K.; Lee, K. J.; Cheon, J. Y.; Lee, J. H.; Joo, S. H.; Moon, H. R. *J. Am. Chem. Soc.* **2013**, *135*, 8940.
(51) Xu, X.; Cao, R.; Jeong, S.; Cho, J. *Nano Lett.* **2012**, *12*, 4988.
(52) deKrafft, K. E.; Wang, C.; Lin, W. B. *Adv. Mater.* **2012**, *24*, 2014.
(53) Deng, Q. X.; Wei, M. D.; Ding, X. K.; Jiang, L. L.; Ye, B. H.; Wei, K. M. *Chem. Commun.* **2008**, 3657.
(54) Bokhimi, X.; Morales, A.; Novaro, O.; Lopez, T.; Chimal, O.; Asomoza, M.; Gomez, R. *Chem. Mater.* **1997**, *9*, 2616.
(55) Chui, S. S. Y.; Lo, S. M. F.; Charmant, J. P. H.; Orpen, A. G.; Williams, I. D. *Science* **1999**, *283*, 1148.
(56) Kondo, A.; Takanashi, S.; Maeda, K. *J. Colloid Interface Sci.* **2012**, *384*, 110.
(57) Jolley, J. G.; Geesey, G. G.; Hankins, M. R.; Wright, R. B.; Wichlacz, P. L. *Appl. Surf. Sci.* **1989**, *37*, 469.
(58) Courcot, D.; Gengembre, L.; Guelton, M.; Barbaux, Y.; Grzybowska, B. *J. Chem. Soc. Faraday Trans.* **1994**, *90*, 895.
(59) Lopez, G. P.; Castner, D. G.; Ratner, B. D. *Surf. Interface Anal.* **1991**, *17*, 267.
(60) Wu, H.; Simmons, J. M.; Liu, Y.; Brown, C. M.; Wang, X. S.; Ma, S.; Peterson, V. K.; Southon, P. D.; Kepert, C. J.; Zhou, H. C.; Yildirim, T.; Zhou, W. *Chem.—Eur. J.* **2010**, *16*, 5205.
(61) Gregg, S. J.; Sing, K. S. W. *Adsorption, surface area, and porosity*; 2nd ed.; Academic Press: London, 1982.
(62) Dubinin, M. M. *Chem. Rev.* **1960**, *60*, 235.
(63) Horvath, G.; Kawazoe, K. *J. Chem. Eng. Jpn.* **1983**, *16*, 470.
(64) Barrett, E. P.; Joyner, L. G.; Halenda, P. P. *J. Am. Chem. Soc.* **1951**, *73*, 373.
(65) Brunauer, S.; Emmett, P. H.; Teller, E. *J. Am. Chem. Soc.* **1938**, *60*, 309.